NTNU

Norwegian University of
Science and Technology

Aerodynamic properties of textiles

Lars Morten Bardal

Master of Science in Energy and Environment
Submission date: June 2010
Supervisor: Lars Sætran, EPT
Co-supervisor: Luca Oggiano, EPT

Norwegian University of Science and Technology
Department of Energy and Process Engineering

Problem Description

Measurements and goals
Define a roughness parameter which is able to describe the surface structure of the textiles.
PIV measurements on 10cm and a 5cm diameter cylinder vertically mounted in the wind tunnel. 6 different textiles will be mounted on each cylinder (3 wool and 3 polyester). Each of the textiles has a different tightness. A tighter textile will result then to have smaller openings and consequently a higher roughness.
HOW WIRE measurements on 10cm and a 5cm diameter cylinder. These measurements will be carried out in order to evaluate the boundary layer and find possible correlations between drag, roughness and friction coefficient.
All the experiments will be carried out on the small wind tunnel at the NTNU department which is able to reach a speed of approximately 20m/s.

Assignment given: 20. January 2010
Supervisor: Lars Sætran, EPT

Aerodynamic Properties of Textiles

Lars Morten Bardal
Norwegian University of Science and Technology
Department of Energy and Process Engineering

Abstract

The aerodynamic drag force acting on a circular cylinder clad with knitted wool and polyester textiles has been investigated in wind tunnel experiments in this study. Particle image velocimetry (PIV) was utilized to determine the flow field, both around the separation point and a wake profile in the close wake. The drag forces and the characteristic C_D curves were determined over a range of Reynolds numbers expected to contain flow transition, for a number of knitted textiles having different surface roughness characteristics. The effects of knitting parameters and type of yarn on the flow field were investigated. The parameters of interest to be examined were critical Reynolds number, separation point, growth of the wake and wake profile. The wool and polyester textiles examined showed dissimilar effects on the flow field. Both were clearly adding surface roughness, and hence tripping transition to turbulence at a lower Reynolds number than for the smooth cylinder. The wool textile did however turn out be a more effective turbulence trigger than expected.

1 Introduction

Aerodynamic properties of textiles have been investigated in several recent studies related to sport science (Brownlie, 1992; Oggiano et al., 2004). The purpose of these studies is mainly to optimize sports garments in order to minimize the drag force acting on athletes performing in high speed sports such as speed skating, cycling etc. This has resulted in the introduction of apparel with zoned fabrics in several sports. In most of this recent research the physical properties of the textiles have not been quantified and systematically used as a parameter however. In order to customize aerodynamic sports apparel to a given event or athlete, more detailed knowledge and systematic data on the aerodynamic properties of different types of fabric, including yarn composition, textile manufacturing techniques and textile manufacturing parameters needs to be acquired.

The total drag force D acting on an arbitrary body can be expressed as

$$D = 0{,}5 \cdot \rho \cdot U^2 \cdot A \cdot C_D$$

where ρ is air density, U is velocity, A is frontal area projected in the direction of U and C_D is the drag coefficient which depends on the shape and surface properties of the body. In order to reduce drag without altering the frontal area of the athlete one therefore need to reduce the drag coefficient itself. The total drag coefficient can be written

$$C_D = C_p + C_f$$

were subscript p and f indicate pressure drag and skin friction drag respectively. For a human body the pressure drag is by far the dominant component due the bluff shape of the torso and the limbs. Achenbach (1968) found the contribution of the skin friction to the total drag on a smooth cylinder to be close to 1-2% in the range of Reynolds numbers considered here. Even though the influence is expected to be higher for a rough surface the contribution is still considered secondary to the pressure drag. Since about 1/3 the total drag on a speed skater or downhill skier is caused by the lower legs (Oggiano and Sætran, 2009) it is obviously a high potential for total drag reduction around the limbs. For simplicity the limbs of a human body can be modelled as circular cylinders. It must however be considered that the distance between the limbs affects the drag coefficient (Oggiano and Sætran, 2009; Pugh, 1970).

For a bluff body the curvature of the surface will accelerate the flow on the frontal surface causing a pressure drop and a favourable pressure gradient. Along the posterior surface the accelerated flow will expand and decelerate causing an adverse pressure gradient. Eventually the low boundary layer momentum can not overcome this pressure gradient, and a reversed flow will appear close to the body. This will cause the flow to separate from the surface, and a large low pressure wake will appear behind the body for all Reynolds numbers in the order of magnitude of interest to sports apparel aerodynamics. The separated flow will increase the total drag dramatically and it is therefore desirable to delay the flow separation and thereby reduce the size of the wake.

Fluid flow around bluff bodies, like a human leg or a circular cylinder, is characterized by a succession of flow transitions from a laminar to a turbulent flow regime respectively in the wake, the free shear layer and in the boundary layer regions. Wieselsberger (1922) showed that the drag coefficient C_D of a cylinder was dependent on the Reynolds number, and that a drop in drag coefficient at high Reynolds numbers called 'drag crisis' was related to the transition to turbulence in the boundary layer around the separation point. This study also pointed out that the transition in the boundary layer was affected by surface roughness. The flow transitions of an idealized disturbance-free flow around a two dimensional cylinder is now found to be dependent on the Reynolds number as a single governing parameter (Zdravkovich, 1990). Each transition state is found to be very sensitive to disturbances in the flow however. Hence in more practical cases the flow transition depends on many influencing parameters. Dependent on their magnitude these disturbance parameters can become governing for the flow transitions. Typical influencing parameters for the flow around a cylinder are free steam turbulence, aspect ratio, space boundaries, oscillations and surface roughness (Zdravkovich, 1997). Each of these influencing parameters can be further divided into separate influencing parameters.

With respect to aerodynamic performance of sports garment and textiles in general the most important influencing parameter is surface roughness. The influence of surface roughness on the flow can be divided in two sub-parameters, relative roughness k/D, and the texture of the roughness.

(Fage and Warsap, 1929) studied the effect of surface roughness on a cylinder and showed that an increasing surface roughness would shift the drag crisis to a lower Reynolds number. Their results also showed that the rougher surface also would generate a smaller drop in C_D than the smoother surface, suggesting that the drag crisis would disappear for very rough surfaces. Achenbach (1970) confirmed these findings and showed that the drag was directly related to the separation angle using skin friction probes to locate the separation point. He also showed that the flow regime of the boundary layer was decisive for the separation angle, and explained this by the increased momentum of the turbulent boundary layer compared to the laminar boundary layer. At $C_{D\ minimum}$ he found a laminar separation followed by a turbulent reattachment, a so-called separation bubble. Also doing measurements in the transcritical domain he found an increase in C_D following the surface roughness. Güven et al. (1980) also did boundary layer measurements on rough cylinders showing the boundary layer growth.

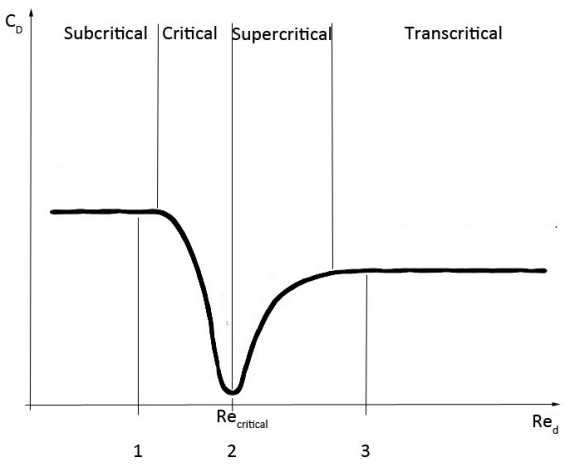

Figure 1 The domains of a typical C_D-Reynolds curve with the velocities used for PIV measurements marked

The use of surface roughness in sports garment is relatively new and the first skin suits used were smooth in order to reduce the frictional drag. Van Ingen Schenau (1981) showed that a rough woollen suit actually had less drag than a smooth speed skating skin suit at low speeds (<6-7m/s) and explained this by an earlier development of a turbulent boundary layer due to the roughness. However speed skating skin suits stayed uniformly smooth for many years. Brownlie (1992) did an extensive study of the use of uniform surface roughness in sports apparel and developed a protocol for individual selection of fabrics for sports apparel. All kinds of textiles will have a natural surface roughness dependent on their method of manufacturing, being weft, knitted or felted. In terms of controlling the roughness of the textile during manufacturing, knitted textiles are suitable due to easily controllable manufacturing parameters such as fibre thickness and stitch length. Controlled variation of these parameters will imply a distinct variation in the appearance of the textile and the surface roughness.

Though the effects of surface roughness in general are well described, the characteristics of the roughness itself also play an important role, influencing how effective the roughness is working as a turbulence trigger and how it effects the growth of the boundary layer. For textiles the surface characteristics are dependent on

- Yarn/fibre composition
- Thickness of the yarn, Tex
- Tightness, Cover factor
- Porosity
- Fabric construction technique

where Tex is a measure for weight per length of yarn and Cover factor (CF) is a measure for the tightness of the fabric defined as

$$CF^2 = \frac{Tex}{L^2}$$

for plain knit fabrics, where Tex is given in grams per km and L is the stitch length given in mm (Spencer, 2001). Since the cover factor links yarn and knit parameters to a single physical fabric parameter, it is used as the variable fabric parameter in this study.

The textiles used in this study are all knitted in a plain stockinette pattern also known as plain knit, which is the most basic weft-knit pattern. Knitted textiles are often preferred over weft textiles for use in sports garment due to their ability to stretch, and thereby fit closely to the body. Weft textiles are not able to stretch in the normal directions of the threads unless elastic yarn is used. Another favourable feature of knitted textiles is the good insulation due to the air pockets in the fabric. In aerodynamic sports garment these properties are appreciated.

The type of yarn used in the textiles is also of great importance for both comfort and aerodynamic performance of the garment. In this study yarn made from wool and polyester were chosen due to their dissimilar physical appearance and their common use in sports garment. While polyester yarn as a plastic has a fairly uniform surface wool yarn is characterized by loose fibres ends extending from the thread. The tiny fuzzy fibres extending from the surface of the knitted wool fabric in an arbitrary fashion can be compared with the fuzz covering a tennis ball. Several studies have been performed on the drag effects of tennis balls. Metha and Phallis (2004) performed drag measurements on tennis ball over a large range of Reynolds numbers (80000-300000) and observed no sudden reduction in C_D as expected for a rough sphere. Hence they suggested that the flow was already in the transcritical flow regime and that the fuzz (loose fibres) covering the tennis ball was a much more effective boundary layer trigger than expected. The article suggested that the individual fuzz filaments themselves caused an additional pressure drag they called “fuzz drag”. The dimensions of the fibres also indicate that they will have a higher C_D (in the region of 3) due to the lower Re_D. The study estimated the influence of the fuzz on the total drag to be as high as 20-40%. In the transcritical flow regime C_D is expected to be essentially independent of R_e as

the transition point has reached the stagnation point, but a reduction of C_D was observed. Both Metha and Phallis (2004) and Goodwill et al. (2003) suggested that this reduction was caused by the wind streamlining and pushing the fuzz down, and hence reducing the "fuzz drag". This theory was supported by Alam et al. (2004). Alam et al. (2007) found that the effect of the fuzz covering a tennis ball had significant and varying influence on the drag at different speeds and probably was dependent on Reynolds effects. The experimental results showed a much lower drag reduction with increasing speed compared to CFD data of a simplified tennis ball without fuzz. The results also showed high scattering of the CD data at low speeds. The study also pointed out the difficulty of measuring aerodynamic effects at low speeds due to the data acquisition sensitivities and relatively high signal noise level. In this study PIV analysis were therefore performed, in addition to traditional drag force measurements, in order to get an impression of the separation point and wake profile impact of the different textiles.

2 Experimental setup

2.1 – PIV

The Particle image velocimetry (PIV) method was utilized to acquire quantitative measurements of the flow field both along the cylinder surface and in the flow wake. This method allows discrete acquisition of the instantaneous velocity field of a fluid flow in two dimensions. The development of digital high speed CCD cameras in the 1990s made the method a valuable tool for fluid mechanics research, and the technique has during the last years been further developed to meet the demands for high accuracy quantitative flow field determination. The basic concept is based on the infinitesimal movement of small seeding particles illuminated by a thin laser light sheet. The particles positions are recorded at time=t and t+Δt by a camera, either on one or two frames. The average movement of fluid in a small interrogation area, containing a sufficient number of identifiable particles, can then be determined using a cross correlation method. Detailed information about the PIV method can be found in I. Grants PIV-review (Grant, 1994). An important assumption of the method is that the seeding particles follow the fluid flow. For gas flows it is therefore a requirement that the particles are very small and approximately neutrally buoyant.

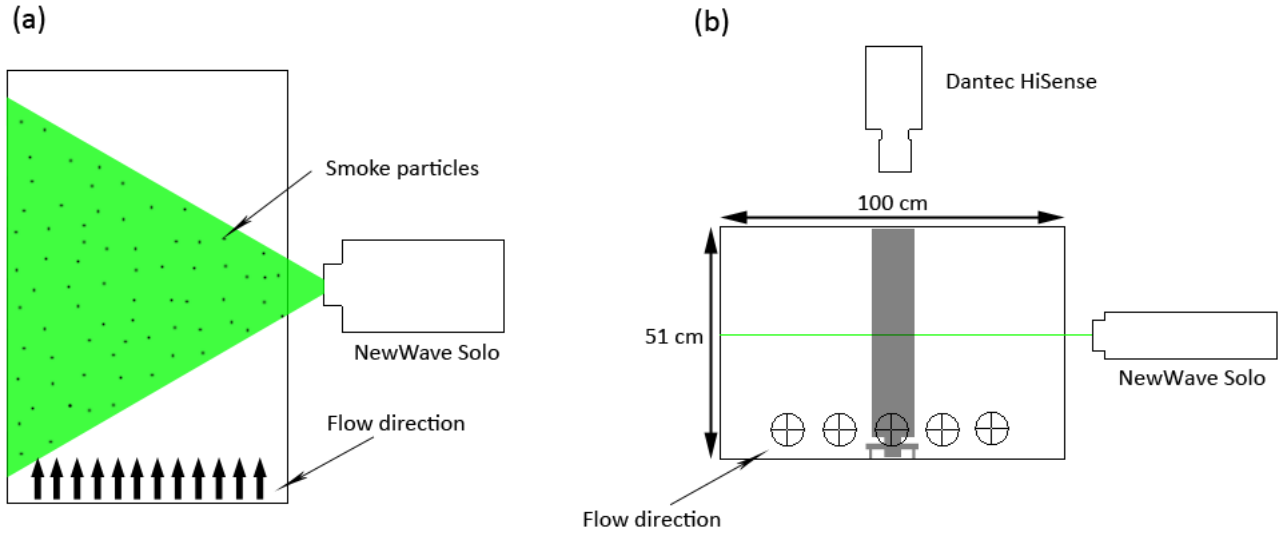

Figure 2 PIV setup (a) top view (b) stream wise view

This means that a high power light source is needed to make a sufficient illumination of each individual particle. For this experiments a Solo Nd:YAG laser from NewWave Research was used to create a thin laser light illumination sheet. The laser sheet was oriented horizontally, parallel with the flow. A Dantec Dynamics FlowSense M2 10 bit high-speed digital camera equipped with a Nikon Nikkor 60mm F2.8D lens was mounted above the wind tunnel roof perpendicular to the laser sheet (see
Figure 2).
Two single exposure frames were captured for every measurement, and the image pairs were analyzed with FlowManager 4.70 software from Dantec Dynamics using an adaptive correlation method with a final interrogation area of 32*32 pixels. The resolution of the camera CCD of 1600*1186 pixels and an interrogation area overlap of 50%, resulting in 99*73 velocity vectors per image, gave a spatial resolution of approximately 1mm. A 40 cm long PVC cylinder was fixed to a steel rail by a rigid 25mm steel rod fixed in both ends of the cylinder to reduce oscillation effects. The cylinder support allowed the cylinder to be shifted in the transversal direction, and the camera was placed on a trolley construction able to move the camera relative to the cylinder in the longitudinal direction. The PIV measurements were conducted in medium sized closed circuit wind tunnel with cross sectional dimensions of 0,51(h) × 1,00(w) meters. The blockage ratio of the setup is defined as d/B where d is the cylinder diameter and B is the width of the test section. The blockage ratio in this case was calculated to be 0,127. This value is around the 0,1 limit under which blockage is usually ignored (Zdravkovich, 2003a), so due to the high Reynolds numbers blockage was not considered in this study.

2.2 - Drag measurements

Drag measurements were performed in the large scale 220 kW wind tunnel in at the department of energy and processing at NTNU, Trondheim. The tunnel is a closed circuit construction with test section dimensions of 12,5(l) × 1,8,(h) × 2,7(w) meters. The resulting blockage ratio is 4% for the largest diameter and was hence disregarded. The drag force component was measured by a Schenck six-way wind tunnel force balance, the free-stream speed was measured with a pitot pressure probe connected to a pressure transducer, and the acquired voltages were logged with a custom LabView logging program at 100Hz. A PVC cylinder model was mounted on a steel support which was fixed to the force balance under the test section floor (see Figure 3). A dummy cylinder was mounted above the test cylinder to reduce 3D end effects, but no such arrangement was made under the test cylinder. The support for the dummy cylinder was fixed to the floor of the wind tunnel 26 cm downstream of the test cylinder and it is assumed that the narrow steel profile did not affect the wake flow particularly. The test cylinder was clad with textiles during the experiments and the textile samples were tightly fixed with the technical face outwards, the wales in the vertical direction and the seam on the downstream side of the cylinder. The dummy cylinder was not clad with textiles during any of the experiments.

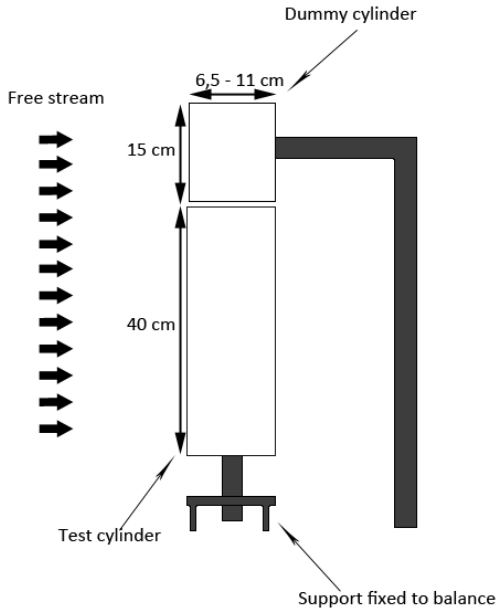

Figure 3 Drag measurement setup

3 Methods

3.1 – Textiles

Wind tunnel experiments were conducted on 40 cm long cylinder models completely clad with textiles, and on smooth PVC cylinders for comparable data. Two different sized cylinders measuring 6.5 cm and 11 cm in diameter were used for the drag measurement tests. All textile samples were fitted to the cylinders with equal tension and consequently the same numbers of wales per cm. This would imply a similar absolute roughness but a higher relative roughness (k/d) for the smaller cylinder. The textile samples were produced at the RMIT University in Melbourne, Australia on a Lawson Hemphill FAK-S knitting machine. This is a laboratory standard knitting machine with a built in stitch control system to ensure a uniform knit sample fulfilling a given stitch length. The textiles used here are the same textiles that were used by Oggiano et al. (2009). It is referred to this article for detailed manufacturing and conditioning details.
The individual textile samples were defined by their cover factor (CF) and their yarn composition. The cover factor is a parameter describing the tightness of the fabric, and by implication how much of the total loop area being covered by the yarn. When CF is increased, either by reducing the stitch length or increasing the thickness of the yarn, the fabric will appear tighter and less perforated. A simple surface analysis was performed using an Epson Perfection 3490 flatbed scanner. Stretched samples of 3,25*3,25 cm were scanned at 2400 ppi and the images were analysed with a custom LabView program. The scanned samples are shown in Table 2. Table 1 shows the correlation found between cover factor and the area covered by yarn, given as percentage of the total area of the sample.

Table 1 Area covered by yarn given in percent

	CF 1,00	CF 1,20	CF 1,40
Polyester	0,6752	0,7373	0,7693
Wool	0,6600	0,7379	0,8049

Table 2 Scanned images of textile samples CF 1.00, CF 1.20 and CF 1.40

	Polyester	Wool
CF 1.00	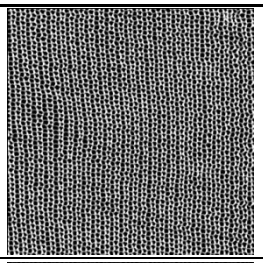	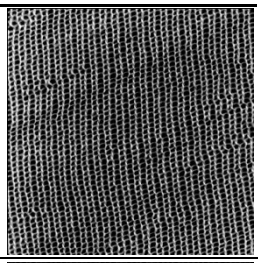
CF 1.20	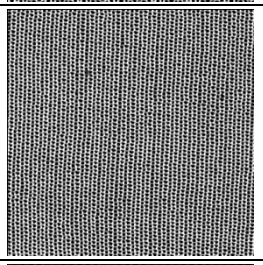	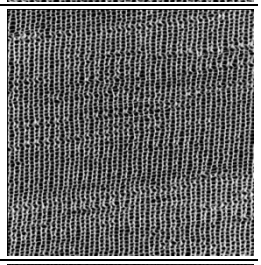
CF 1.40	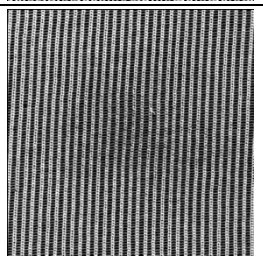	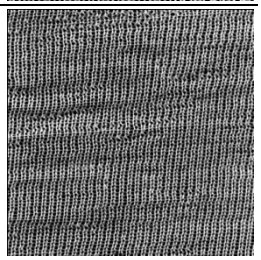

3.2 - Drag force measurements

Drag force measurements were performed for increasing Reynolds numbers to obtain a relation between drag coefficient (C_D) and Reynolds number. The drag force on 5 different textiles samples with varying CF values ranging from 1,00 to 1,40 were measured for both wool and polyester.
The measurements were performed according to the setup described in Figure 3. Ten increasing wind speed measurement points, ranging from 10 to 23,5 m/s, controlled by the rpm of the fan, was used for every measurement series. Samples were taken at a sampling frequency of 100 Hz and a sample time of 20 seconds, resulting in 2000 samples per measurement both for wind speed and drag force. The drag force acting on the support was measured and subtracted from the total force. The average drag force values were then used to calculate C_D values based on the cylinder frontal area.

3. 3- PIV

PIV analysis was used to define how the flow field develops behind the cylinder for the different textiles. Textile samples with a cover factor of 1,25 were chosen for the PIV analysis. All the measurements were also performed on a smooth PVC cylinder for comparable data since much data in literature is based on smooth cylinders.

PIV velocity field measurements were performed at three different velocities. The choice of velocities was based on the shape of the C_D-Re curve for the Polyester CF 1,25 textile sample since the wool textile had no characteristic C_D-drop in the Reynolds range considered. Three characteristic speeds were chosen for the PIV analysis. These are marked in Figure 1. The lowest velocity was subcritical for the polyester textile and located shortly to the left of the transition point in the C_D-Re curve. The medium velocity was critical and located approximately at the low extreme of the C_D-Re curve. The high velocity was assumed to be transcritical and was located at the highest measuring point of the drag measurements, close to the wind tunnel maximum velocity. The measurements were taken in three different sessions and hence there were small variations in the velocities (max 5%).

A measurement series of 5 image series of 60 image pairs were taken along the flow field close to the cylinder surface for each velocity and surface configuration. These image frames included the cylinder surface in order for the separation point to be approximately located and the close wake development to be determined. For quantitative data a reference coordinate system was determined from the tangents of the visible outline of the cylinder surface for each recording. The average flow fields was calculated from 60 image pairs with a total sampling time of 7,5 seconds, and the camera was shifted relative to the cylinder between each measurement.

From the resulting velocity profiles the location of the separation point was manually estimated. These values must be considered approximate since the vector field resolution and light reflections from the fabric surface inhibited accurate readings. The development of the time average vortices in the near wake of the cylinder was quantified as the transverse distance from the cylinder centre axis to the point of zero stream wise velocity as shown in Figure 4. This parameter is used to quantify the development of the wake width, which is influencing the pressure drag induced.

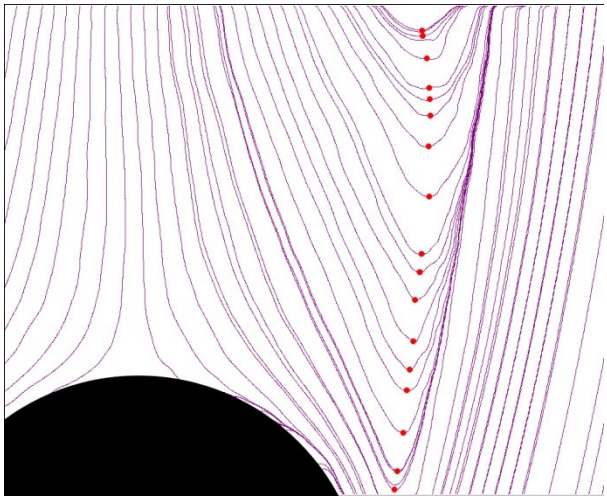

Figure 4 Average flow field streamlines with red wake markers

A second measurement series was performed at a distance downstream of the cylinder in order to determine the near wake velocity profiles. For this series 100 image pairs with a total sampling time of 12,5 seconds were captured per position to ensure a reliable average flow field. The cylinder was shifted in the transversal direction in order to cover the whole wake width, and a total of 7 overlapping images were captured per profile. Velocity profiles for the stream wise velocity component were extracted from the flow field at x/d=3,5, 4 and 4,5 where x is the stream wise position and x=0 is the cylinder centreline. The captured sections of the profiles were then stitched together using Matlab R2009b. Assuming a symmetric velocity profile, a mirror image of the half wake was used to produce the complete profile.

4 Results and discussion

4.1 - Drag measurements

From the acquired drag force data the drag coefficients C_D was calculated and plotted against Reynolds number. The results for the polyester textiles are shown in Figure 5 and Figure 6. The results for the 6,5 cm cylinder covered with polyester textiles seem to correspond well with theory and comparable studies carried out on rough cylinders in the literature (Fage and Warsap, 1929; Achenbach, 1970; Güven et al., 1976). The knitted polyester fabric triggers transition to turbulence in the boundary layer causing a drag crisis at Reynolds numbers well below those expected for smooth cylinders. It seems that the critical Reynolds number, defined in Figure 1, roughly follows the cover factor of the textile in such a way that the looser fabric acts like a rougher surface, and hence triggers transition at a lower Reynolds number. This is shown in detail in Figure 8 where the critical Reynolds number is plotted against the cover factor. With exception of CF 1,20 for the large cylinder and CF 1,00 for the small cylinder the values are increasing with CF. This trend is supported by Oggiano et al. (2009) where a surface analysis of the textiles was performed and a roughness coefficient k_{tex} was defined. That study showed a linear correlation between CF and apparent roughness. Due to the poor resolution of data points no exact correlation can be found from the results in this study.

The C_D-R_e curves found also correspond well to the C_D-R_e curves obtained by Oggiano et al. (2009) although slightly higher C_D values were measured generally in this study. The 11 cm cylinder show similar results, again with exception of the CF 1,20 sample. This deviation may be caused by the fact that this sample was too short to cover the entire cylinder leaving a bare area of smooth PVC over and under the sample. Also the plots clearly show the tendency of a higher $C_{D\,min}$ for the textiles with premature transition as expected and predicted by Fage and Warsap (1929). This is also shown in Figure 7 where the drop of the drag coefficient is plotted against cover factor. The drop in C_D from the subcritical value to $C_{D\,min}$ ranges from 22,4% to 29,2%. This corresponds well to the findings of Oggiano et al. (2009). Again with the exception of the CF 1,20 sample, the data show a clear increasing tendency, although a linear relation can not be confirmed.

For the small cylinder the subcritical C_D values coincide around 1,2 while this value is reduced to around 1,0 for the larger cylinder. Since the drag coefficient, as denoted by Achenbach (1970), should be uninfluenced by roughness in this flow regime, this difference is assumed to be caused mainly by the difference in aspect ratio (Zdravkovich, 2003b) since the bottom end of the cylinder was a free end. This explanation also agrees with the fact that the relative drop in drag was in the same range for both diameters.

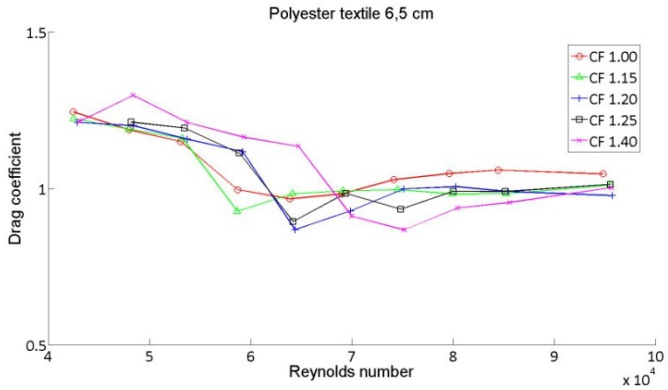

Figure 5 Drag Coefficient vs. Reynolds number for polyester textiles d=6,5 cm

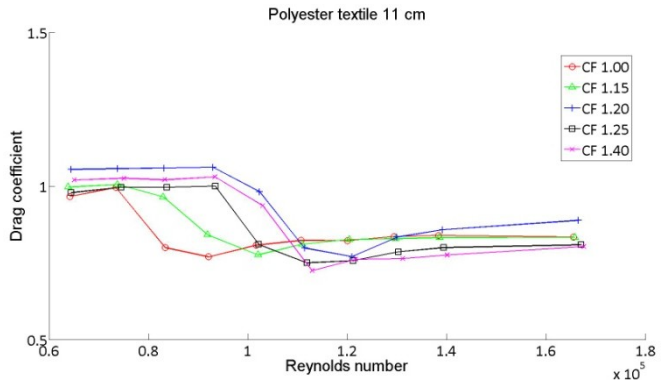

Figure 6 Drag Coefficient vs. Reynolds number for polyester textiles d=11 cm

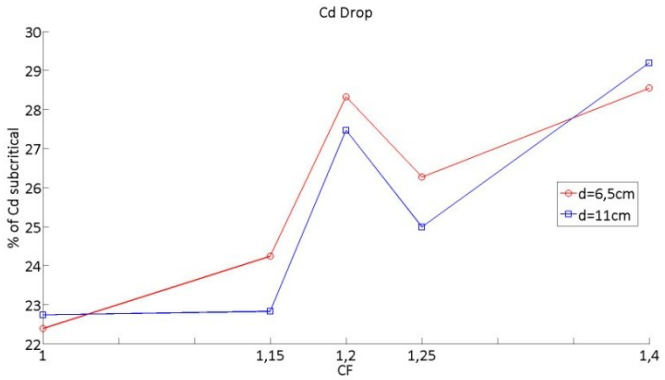

Figure 7 C_D drop given in percent of subcritical value vs. cover factor

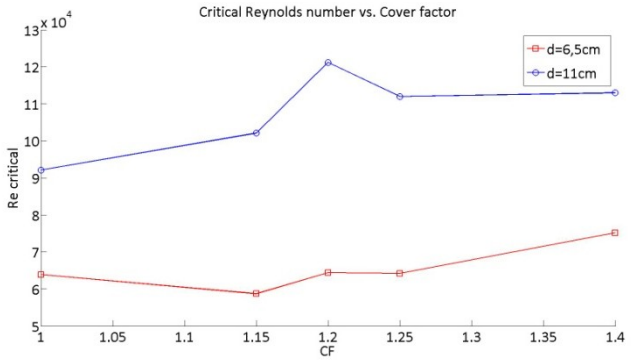

Figure 8 Critical Reynolds number vs. cover factor for polyester textiles d=6,5cm and d=11cm

For the wool textiles the results showed a different behaviour not foreseen. There is also very limited research performed on such textiles to compare the acquired data to. The C_D-Re curves for the wool textiles are shown in Figure 9 and Figure 10. In the range of Reynolds numbers considered ($4\times10^4 - 1{,}7\times10^5$) all the textiles have a fairly constant C_D value for both diameters tested. This means that the wool textiles do not induce a drag crisis in this range of Reynolds numbers. Hence, assuming that the wool acts like a rougher surface than the polyester, transition to turbulence occurs in the boundary layer at even lower Reynolds numbers. This is a similar observation to the one made on flow over tennis balls by Metha and Phallis (2004), and means that the flow is already in the transcritical state. This is an interesting but not all surprising observation since the wool textiles, like the tennis ball felt, has a number of loose fibres extending from the surface. Although these fibres are not as apparent on the textile samples as on tennis balls it is clearly more effective as a boundary layer turbulence trip than the roughness of the corresponding polyester textiles.

The average C_D values of the wool textiles seem to be similar to the subcritical C_D values of the polyester textiles for both cylinder sizes. Since the two fabrics appear to be in two different flow regimes, the excess drag on the wool must be explained. It is expected that C_D will increase in the supercritical region as the boundary layer thickens, hence weakens, and the separation point moves forward. It is therefore possible that the separation point has reached the same position as for the laminar boundary layer of the subcritical polyester textile, creating the same pressure drag. When the whole boundary layer has become turbulent the separation point would no longer move and the drag should no longer be dependent on Reynolds number. C_D would hence be constant like shown in the plots.

Moreover no clear correlation is found between cover factor and drag coefficient for the wool textiles, indicating that other parameters might be more influencing on the drag. The relative high level of noise in the measurements also makes it difficult to draw a clear conclusion from this relationship.

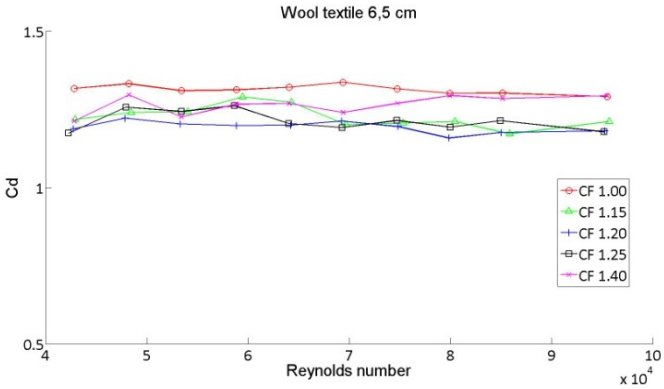

Figure 9 Drag Coefficient vs. Reynolds number for wool textiles d=6,5 cm

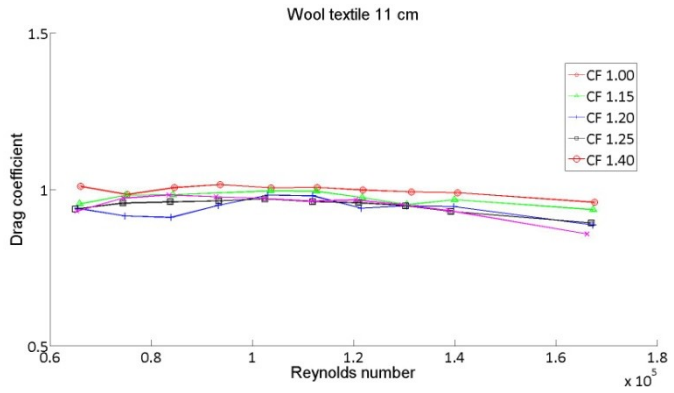

Figure 10 Drag Coefficient vs. Reynolds number for wool textiles d=11 cm

4.2 – PIV measurements

The PIV measurements were preformed in order to clarify the aerodynamic differences between wool and polyester textiles found in the drag measurements. Problems with light reflections from the reflective white surface of the fabrics degraded the accuracy of the flow field near the surface, hence making accurate determination of boundary layer thickness and separation point difficult. At a distance from the cylinder surface the recordings were however capable of reproducing a consistent average flow field. The velocity field vector plots of all configurations in the close wake are shown in

Table 3. It can be observed from the images that both wake expansion and separation point seem to be near constant for wool and smooth PVC at all three velocities. This is expected as C_D is also constant for these configurations in this velocity range. The polyester textile shows a different characteristic. The flow field for the subcritical velocity appears similar to the wool, but when the critical Reynolds number is reached the separation point is moved down stream as predicted from theory. This results in a significant narrower wake with almost zero expansion. When the Reynolds number is further increased the separation point appears to creep upstream again, making the wake broader, however not as broad as in the subcritical regime.

Table 3 Velocity vector field of near wake

	Polyester	Wool	Smooth PVC
Velocity 1	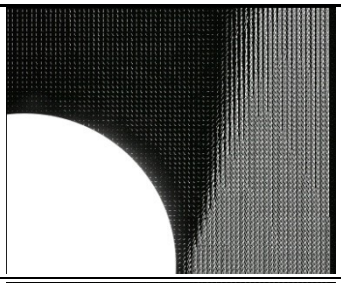	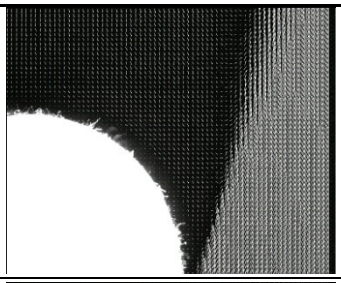	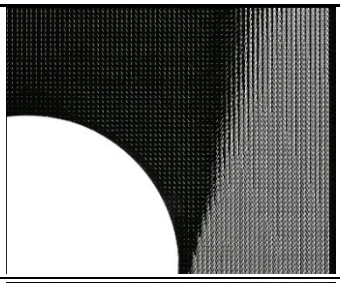
Velocity 2	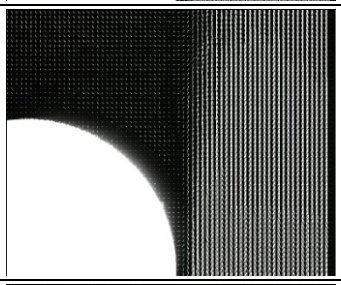	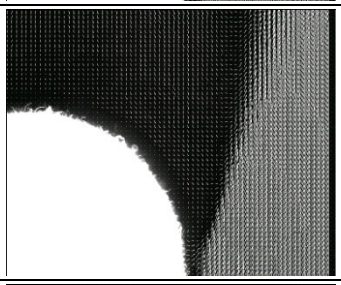	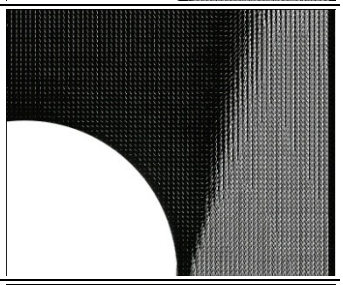
Velocity 3	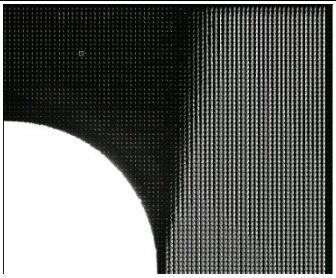	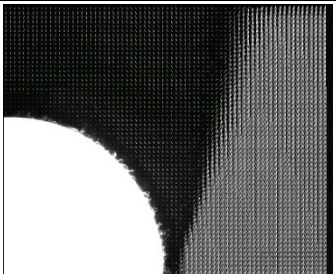	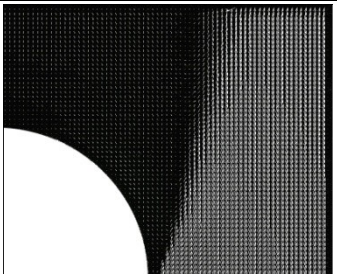

The development of the average vortices in the very near wake is quantified in Figure 11 as explained in Figure 4. As the images in Table 3 indicate, all flows appear to have a similar average wake growth in the region close to the cylinder with exception of the critical Reynolds flow for the polyester. This is the only configuration where the wake width does not increase downstream. The absolute values of the wake width have apparent variation. This would be the result of a shifted separation point. The variations are small (>5% of cylinder diameter) except for the wool textile at the low velocity and the polyester textile at the critical and transcritical velocity. It is somewhat surprising that the polyester actually has a narrower profile at the transcritical velocity than at the critical velocity very close to the cylinder surface. The PVC profile also appears narrower at the high velocity, indicating that wall effects might be influencing. Moreover it is hard to draw a clear conclusion from this.

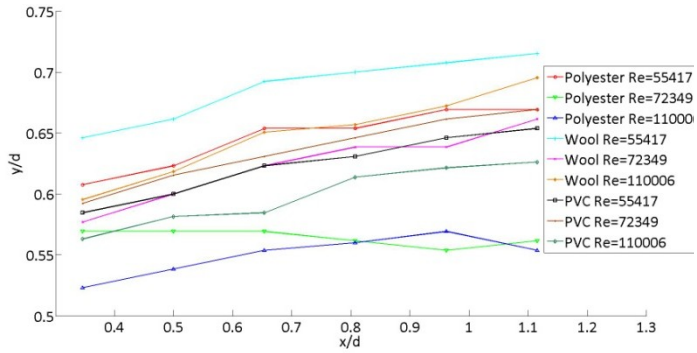

Figure 11 Width of very near wake as defined in figure 4. x is the stream wise position and y is the transversal position. x/d=0 and y/d=0 are cylinder centrelines.

A fixed coordinate system is defined with x as the stream wise position and y as the transversal position. The origin is defined as the cylinder centre. The average near wake velocity profiles at x/d=4 is plotted for polyester in Figure 12, wool in Figure 13 and a smooth PVC cylinder in Figure 14. The profiles are reduced with the terminal velocity at the edge of the wake (U). The polyester shows a large variation in both the shape of the velocity profile and the centreline velocity. The subcritical flow produces an average wake with large gradients in the transversal direction. The reduced centreline velocity is low (11,5% of terminal velocity), but the wake width is actually lower than for the higher velocities. The profile at the critical velocity has the lowest gradients and the highest reduced centreline velocity (67,2% of terminal velocity). The wake profiles seem to correspond well with the data from the drag measurements, with the flattest profile producing the lowest C_D. For the wool textile the reduced velocity profiles plotted in Figure 13 all coincide to approximately the same curve. This corresponds well with the fact that C_D is constant for all velocities. The only deviation found is for the medium velocity which flattens out a little earlier than the other profiles, producing a slightly broader wake. For the smooth PVC cylinder all the profiles coincide to the same curve as expected, also producing a constant C_D in this Reynolds range.

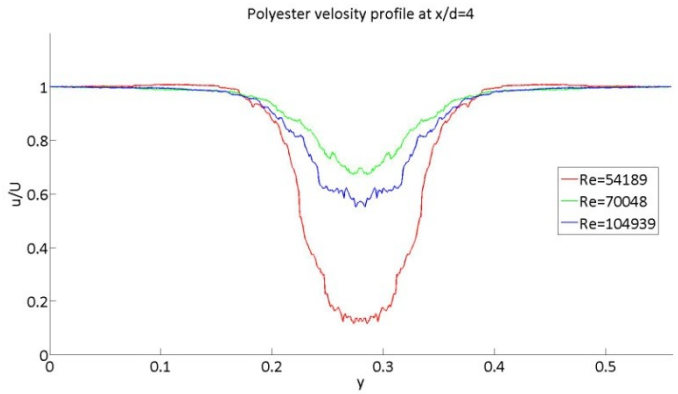

Figure 12 Reduced near wake velocity profiles for polyester textile at x/d=4

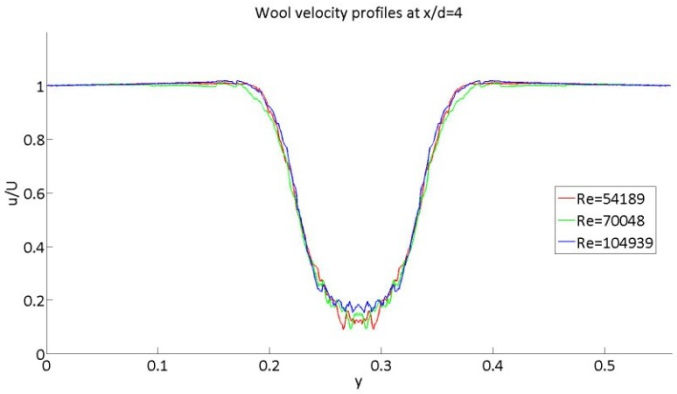

Figure 13 Reduced near wake velocity profiles for wool textile at x/d=4

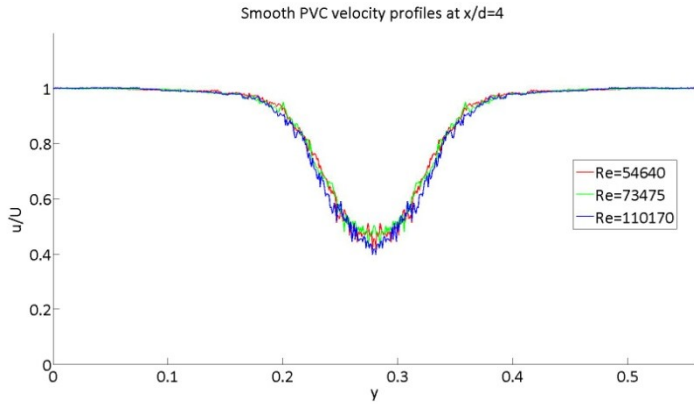

Figure 14 Reduced near wake velocity profiles for smooth PVC cylinder at x/d=4

In order to ease the comparison between the configurations all profiles at the low velocity are plotted together in Figure 15. An interesting observation to be made from this plot is that the subcritical polyester coincides with the transcritical wool in the centre of the wake, but the polyester has higher velocity gradients at the edge of the wake, making the wake narrower. From the drag measurements it was observed that these configurations produced the same C_D at this velocity. The smooth PVC cylinder produces a flatter wake at this velocity, but this wake is also significantly wider than the textile covered cylinders. This shows that the wake is influenced by the surface roughness also in the subcritical regime. A possible explanation is that the surface roughness influences the flow transition in the free shear layers as described by Zdravkovich (1990).

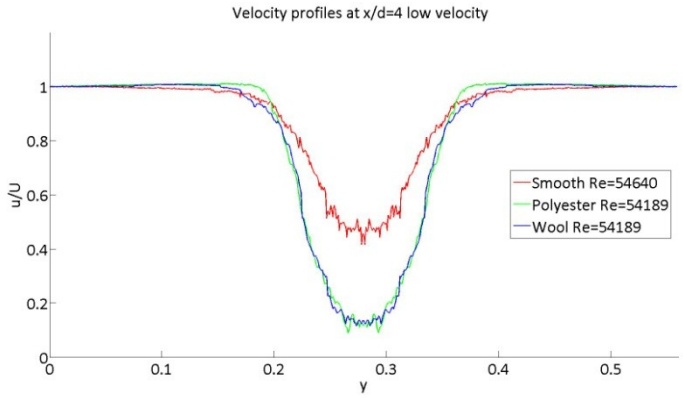

Figure 15 Reduced velocity profiles at low velocities for polyester, wool and PVC

The centreline velocities are plotted against Reynolds number in Figure 16. This shows, as seen from the velocity profiles that while the wool textile and the smooth PVC has approximately constant centreline velocities the polyester textile show large variations due to the boundary layer transition. From Figure 17 the recovery of the centreline velocity in the wake can be observed. There are no noticeable differences in the recovery rate of the centreline mean velocity for any of the configurations tested.

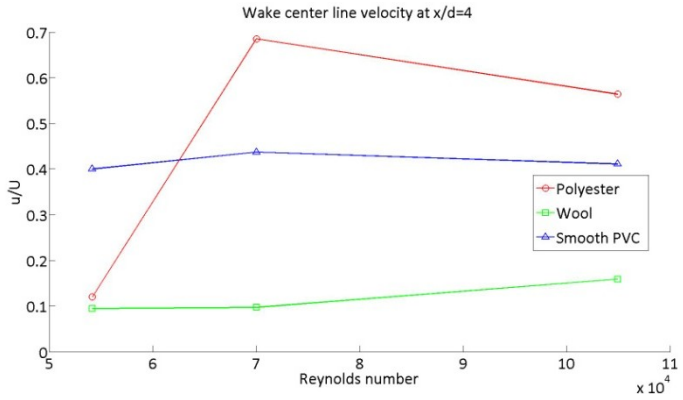

Figure 16 Centre line velocity at x/d=4 for each configuration plotted against Reynolds number

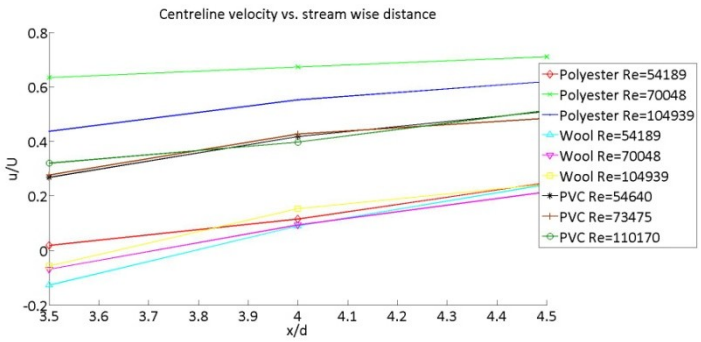

Figure 17 Reduced wake centerline velocity plotted against stream wise distance from x/d=3,5 to x/d=4,5

5 Conclusions

The results in this study support a correlation between textile cover factor, roughness and drag coefficient for knitted polyester textiles found in previous studies. The polyester textiles are effective in triggering premature transition to turbulence in boundary layers, and the critical Reynolds number is found to be directly dependent on cover factor. The wool textiles tested did not show any sign of flow

transition in the Reynolds range tested ($0{,}4\times10^5<Re<1{,}7\times10^5$) and are hence assumed to be in the transcritical flow regime. From this results wool textiles appear to be a much more effective turbulence trigger than polyester textiles. It is presumed that this property is caused by the loose fibres extending from the wool threads. The subcritical flow around the polyester coated cylinder causes was found to cause the same drag coefficient as the transcritical flow around the wool coated cylinder. PIV measurements confirm that the wake profiles of these two flow fields are in fact similar. Compared to a smooth cylinder the polyester textile is advantageous for critical and higher Reynolds numbers while the wool textile is disadvantageous in the whole Reynolds range considered.

References

- Achenbach E. (1968) Distribution of local pressure and skin friction around a circular cylinder in cross-flow up to *Re* = 5×10^6, Journal of Fluid Mechanics; Vol. 34, part 4, pp. 625-639
- Achenbach E. (1970) Influence of surface roughness on the cross-flow around a circular cylinder, Journal of Fluid Mechanics; Vol. 46, part 2, pp. 321-335
- Alam F., Watkins S., Subic A. (2004) The aerodynamic forces on a series of tennis balls, 15th Australasian Fluid Mechanics Conference, The University of Sydney, Sydney, Australia
- Alam F., Tio W., Watkins S., Subic A., Naser J. (2007) Effects of spin on tennis ball aerodynamics: An experimental and computational study, 16th Australasian Fluid Mechanics Conference Crown Plaza, Gold Coast, Australia
- Brownlie L.W. (1992) Areodynamic characteristics of sports apparel, Doctoral Dissertations, Simon Fraser University, Burnaby, B.C., Canada
- Fage A., Warsap J.H. (1929) The effects of turbulence and surface roughness on the drag of a circular cylinder, Aeronautical Research Committee, Reports and Memoranda No. 1283
- Goodwill S.R., Chin S.B., Haake S.J. (2003) Aerodynamics of spinning and non-spinning tennis balls, Journal of Wind Engineering and Industrial Aerodynamics; Vol. 92 pp. 935–958
- Grant I. (1994) Particle image velocimetry: a review, Proceedings of the Institution of Mechanical Engineers, Part C: Journal of Mechanical Engineering Science; Vol 211(1) pp. 55-76
- Güven O., Farell C., Patel V.C. (1976) Surface-roughness effects on the mean flow past circular cylinders, Journal of Fluid Mechanics; Vol 98(4) pp. 673-701
- Metha R.D., Phallis J.M. (2004) Tennis ball aerodynamics and dynamics, Biomedical Engineering Principles in Sports, Kluwer Academic/Plenum Publishers, ISBN 0 306 48477 3, pp. 99-123
- Oggiano L., Troynikov O., Konopov I., Subic A., Alam F. (2009) Aerodynamic behaviour of single sport jersey fabrics with different roughness and cover factors, Sports Engineering; Vol. 12.(1) pp. 1-12
- Oggiano L., Sætran L., Løset S., Winther R. (2004) Reducing the athletes's aerodynamical resistance, Journal of Computational and Applied Mechanics; Vol. 5(2) pp. 1-8
- Oggiano L., Sætran L. (2009) Experimental analysis on parameters affecting drag force on athletes, The impact of Technology on Sport; Vol. 3 pp. 383-389
- Pugh L.G.C.E. (1970) The influence of wind resistance in running and walking and the mechanical efficiency of work against horizontal or vertical forces, Journal of Physiology 213 (2), pp. 255-276

- Spencer D.J. (2001) Knitting technology: a comprehensive handbook and practical guide, Woodhead Publishing Limited, ISBN 1 85573 333 1
- Van Ingen Schenau G.J. (1981) The influence of air friction in speed skating, Journal of Biomechanics; Vol. 15(6), pp. 449 458
- Wieselsberger C. (1922) New data on the laws of fluid resistance, Physikalishe Zeitschrift; Vol. 22
- Zdravkovich M.M. (1990) Conceptual overview of laminar and turbulent flows past smooth and rough circular cylinders, Journal of Wind Engineering and Industrial Aerodynamics; Vol. 33 pp. 53-62
- Zdravkovich M.M. (1997) Flow around circular cylinders Vol. 1: Fundamentals, Oxford University Press, ISBN 0 19 856396 5, pp. 3-8
- Zdravkovich M.M. (2003a) Flow around circular cylinders Vol. 2: Applications, Oxford University Press, ISBN 0 19 856561 5, p. 827
- Zdravkovich M.M. (2003b) Flow around circular cylinders Vol. 2: Applications, Oxford University Press, ISBN 0 19 856561 5, p. 742